Available online at www.sciencedirect.com

Metabolism

www.metabolismjournal.com

Dual pathways of p53 mediated glucolipotoxicity-induced apoptosis of rat cardiomyoblast cell: activation of p53 proapoptosis and inhibition of Nrf2-NQO1 antiapoptosis

Hye Jin Wang[a,1], Eun Young Lee[b,1], Seung Jin Han[c], Soo Hyun Kim[b], Byung-Wan Lee[b], Chul Woo Ahn[a,b], Bong Soo Cha[a,b], Hyun Chul Lee[a,b,*]

[a] Brain Korea 21 Project for medical science, Seoul, Korea
[b] Department of internal medicine, Yonsei University College of medicine, Seoul, Korea
[c] Department of endocrine and Metabolism, Ajou University School of Medicine, Seoul, Korea

ARTICLE INFO

Article history:
Received 10 November 2010
Accepted 15 September 2011

ABSTRACT

Reactive oxygen species (ROS), driven by excessive levels of glucose and free fatty acids, appears to induce cell apoptosis. However, the underlying molecular mechanism of this process remains unclear in cardiac myocytes. We investigated the glucolipotoxicity effects of high glucose and palmitic acid (C16:0) on the rat cardiomyoblast cell line (H9c2) focusing on tumor suppressor p53. Cultured H9c2 rat cardiomyoblasts were exposed to palmitate and/or to an elevated glucose concentration for 18 hours. Only the glucolipotoxic condition of 30 mM glucose in combination with 250μM palmitate resulted in significant generation of ROS and upregulation of p53 which caused to an increased cleavage of caspase-3. On the other hand, the expression of NF-E2-related factor 2 (Nrf2) showed increased tendency while the expression of NAD(P)H: quinone oxidoreductase-1 (NQO1) was decreased. N-acetyl L cysteins and pifithrin-α, an inhibitor of p53 abrogated glucolipotoxicity-induced ROS generation and p53 expression. Chromatin immunoprecipitation analysis revealed that p53 interacted antioxidant responsive elements (ARE)-containing promoter of NQO1. Upregulated p53 counteracted the Nrf2-induced transcription of ARE-containing promoter of NQO1 gene and leaded to decrease in NQO1 expression. We demonstrated that the elevated p53 mediated glucolipotoxicity-induced apoptosis of rat cardiomyoblast cell through dual pathways: stimulating pro-apoptosis signaling as well as suppressing anti-apoptosis pathway of Nrf2-NQO1 signaling.

1. Introduction

Several tissue specific cellular damages, induced by reactive oxygen species (ROS), have been implicated under the condition of excessive levels of glucose and free fatty acids [1-3]. The glucolipotoxicity-induced oxidative stress is reported to play key roles in apoptosis. However, the underlying molecular mechanism of apoptosis remains unclear especially in cardiac myocytes.

Author contributions: Hye Jin Wang: performed research and wrote the paper. Eun Young Lee: analyzed data, and wrote the paper. Seung Jin Han: designed research. Soo Hyun Kim: performed research. Byung-Wan Lee: collected and analyzed data, and wrote the paper. Chul Woo Ahn & Bong Soo Cha: did data interpretation Hyun Chul Lee: designed research, performed research and wrote the paper.

* *Corresponding author*. Department of internal medicine, Yonsei University College of Medicine, 250 Seongsanno, Seodaemun-Gu, Seoul, 120-752, Republic of Korea. Tel.: +82 2 2228 1943.
E-mail address: endohclee@yuhs.ac (H.C. Lee).

[1] These authors were equally contributed in this journal by first authors.

0026-0495/$ – see front matter © 2012 Elsevier Inc. All rights reserved.
doi:10.1016/j.metabol.2011.09.005

Not only DNA damage but also accumulation of intracellular ROS can increase p53 expression [4], which regulates the expression of many genes to arrest cell cycle for allowing time for DNA repairing and finally induces cell apoptosis [5]. In addition, p53 is known to bind to the antioxidant response element (ARE) of many ROS scavenging and detoxification enzymes such as NAD(P)H: quinone oxidoreductase-1(NQO1) and glutathione S-transferases [6], leading to decrease in expressions of antioxidant enzymes. Therefore, p53 can inhibit NF-E2-related factor 2 (Nrf2)-induced transcription of antioxidant enzymes by competitive binding to ARE under ROS stress [6]. In these regards, we hypothesized that p53-Nrf2/ARE pathway might be another mechanism of glucolipotoxicity-induced apoptosis in H9c2 cells. To demonstrate this hypothesis, we investigated whether p53 might play dual roles in glucolipotoxicity-induced cell apoptosis in a rat cardiomyoblast cell line.

2. Methods

2.1. Study design

To demonstrate our hypothesis, cultured H9c2 rat cardiomyoblasts were exposed to palmitate and /or to an elevated glucose concentration. After 18 hours, cell survival and apoptosis were determined by MTT assay and Annexin V-PI staining, respectively. ROS generation was studied to verify oxidative stress. To investigate the role of p53 in glucolipotoxicity-induced cell apoptosis, cultured cells was treated with pifithrin-α, a p53 inhibitor, and p53 siRNA. Western blotting was used to study p53, NQO1, Nrf2, cleaved caspase-3, and β-actin. Chromatin immunoprecipitation assay was used to assess p53-ARE interaction.

2.2. H9c2 cells culture and treatment with glucose and palmitic acid

H9c2 rat cardiomyoblasts were maintained at 37°C, 5% CO_2 in DMEM/F-12 (WelGENE, Daegue, South Korea) supplemented with 10% bovine calf serum (WelGENE, Daegue, South Korea), penicillin (100U/ml), and streptomycin (100μg/ml). H9c2 cells were incubated in DMEM/F12 media (normal glucose: 5 mM, high glucose: 30 mM) with 0.25% (wt/vol) BSA alone (control) or 0.25 mmol/l palmitate complexed to 0.25% (wt/vol) BSA for 18 h. Preparation of the 0.25 mmol/l palmitic acid media was carried out as previously described [7].

2.3. Cell survival assays

MTT [3-(4,5-dimethylthiazol-2-yl)-2,5-diphenyl-tetrazolium bromide] assay was used to determine cell viability following the manufacturer's protocols. H9c2 cells were dispensed in 24-well plates at a density of 5×10^4 cells/well. The cells were treated with MTT (0.5 mg/ml) for 4 h at 37°C and then dissolved in 250μl DMSO. After 30 min at room temperature, absorbance was measured at 540 nm using a microplate reader (Molecular Devices, Palo Alto, CA).

2.4. Annexin V-PI staining

For detection of phosphatidylserine externalization by flow cytometry, Annexin V-FITC (AV, BD Biosciences, San Diego, CA)/PI assay was used. Briefly, after treatment with reagents, 5×10^5 cells were harvested and washed with ice-cold PBS and then incubated in 100 ml of buffer containing AV and PI for 15 min at room temperature. The cells were immediately analyzed by flow cytometry on a FACScan (Becton Dickinson Heidelberg, Germany). Cells were considered early apoptotic when they were AV-positive but PI-negative and late apoptotic when they were both AV- and PI-positive.

2.5. Knockdown and inhibition p53

For inhibition and knockdown of p53 expression in response to glucolipotoxicity, cultured cells was treated with PFTα, a p53 inhibitor, or trasnfected H9c2 cells with siRNA molecules against rat p53 (sc-45917, Santa Cruz Biotechnology, Santa Cruz, CA) in the presence or absence of 0.25 mmol/l palmitate and 30 mM high glucose. The sense and antisense sequences of rat p53 were as follows: 5′-TATGTCTAAGGGACCTGCGGTT GGCATTGATCTTG-3′ and 5′-GTGCCAAGATCAATGCCAACCG CAGGTCCCGGAGACA-3′. The p53 0.01 mmol/l siRNA were transiently transfected into differentiated H9c2 cells with Lipofectamine 2000 according to the manufacturer's instructions (Invitrogen, Carlsbad, CA) for 18 h. For enzymatic inhibition of p53 expression, p53 competitive inhibitor, PFTα was dissolved in DMSO to the final concentration of 0.1 mmol/l.

2.6. Detection of ROS

Intracellular ROS generation was assessed by flow cytometry following staining with 10 mmol/l 6-carboxy-2′,7′-dichlorodihydrofluorescein diacetate (H_2DCFDA) (Invitrogen, Oregon, USA). Cells ($2X10^5$ cells/60 mm dish) were treated with 5μM H_2DCFDA. After 30-min incubation at 37°C, cells were examined under a fluorescence microscope set at 488 nm for excitation and 530 nm for emission, and sorted by flow cytometry.

2.7. Preparation of nuclear and cytoplasmic extracts

H9c2 cells were washed and incubated for 10 min with ice-cold PBS, scraped into PBS with 1 mM phenymethylsulphonyfluoride (PMSF), and pelleted by centrifugation (500 *g*) at 4°C for 10 min. Cell pellets were resuspended in buffer A (20 mM HEPES, pH 7.9, 10 mM KCl, 0.1 mM ethylenediamine tetraacetic acid (EDTA), 1 mM ethyleneglycol tetraacetic acid (EGTA), 1 mM sodium orthovanadate, 50 mM NaF, 1 mM PMSF, 20 mg/ml aprotinin, 20 mg/ml antipain, 20 mg/ml leupeptin and 10 mg/ml pepstatin A) and incubated on ice for 10 min. Nonidet P-40 was added to a final concentration of 0.2% and the cell suspension was passed through a 26-gauge needle to break open the cells. After centrifugation (12 000 *g*, in a microcentrifuge) at 4°C for 1 min, supernatants were collected as cytoplasmic extracts, and the pellets (crude nuclei) were resuspended in buffer B (20 mM HEPES, pH 7.9, 0.4 M NaCl, 1 mM EDTA, 1 mM EGTA, 1 mM dithiothreitol (DTT), 1 mM sodium orthovanadate, 50 mM NaF and the same protease inhibitors as in buffer A). After incubating for 60 min on ice, insoluble materials were pelleted

by centrifugation (15 000 *g*) at 4°C for 10 min and supernatants were collected as nuclear extracts.

2.8. Western blot analysis

Whole lysated and nuclear proteins extracts were separated by 12 % SDS-PAGE, blotted onto polyvinylidene difluoride membranes, and detected using the following primary antibodies: p53, NQO1, Nrf2 (Santa-Cruz biotechnology, CA, USA), cleaved caspase-3 (Cell signaling, MA, USA) and β-actin (Sigma-aldrich) antibodies were used as primary antibodies, diluted 1:1000. Horseradish peroxidase-conjugated goat anti-mouse IgG, anti-rabbit IgG and anti-goat IgG (Santa-Cruz biotechnology) were used as secondary antibodies (at dilution of 1:5000). Development of the western blot was performed using an enhanced chemioluminisence western blotting analysis system (Amersham).

2.9. Chromatin immunoprecipitation assay

The H9c2 cells were fixed using 1% formaldehyde in medium for 10 min at room temperature. The cells were treated with 0.125M glycine for 5 min to stop fixation and washed twice with ice-cold PBS. The cells were scraped in PBS, collected by centrifugation, and lysed in lysis buffer. After centrifugation, nuclear pellet was resuspended in nuclear lysis buffer and sonicated for four cycles (30-s pulse and 30-s rest on ice). Sheared chromatins were immunocleared with protein A/G-agarose slurry (Santa-Cruz biotechnology, CA, USA) for 1 h at 4 °C. The immunoprecipitates were washed sequentially with low salt buffer; with high salt buffer; with LiCl buffer; and TE buffer for 5 min each. Protein-DNA complexes were resuspended in TE buffer for reversal of cross-links by heating at 65 °C overnight. Then, DNA was purified using proteinase K treatment at 50 °C for 3 h followed by phenol extraction and ethanol precipitation. PCR was performed using 1:100-diluted input DNA and 3μl of immunoprecipitated DNA from a 30μl sample. The association of p53 with endogenous NQO1 promoter ARE region in H9c2 cells was measured by PCR on immunoprecipitated chromatin using the following primers spanning the NQO1 promoter containing AREs: F;5′-GCAGTTT CTAAGAGCAGAATC-3′ R; 5′-TTAGTCCTTGGTCAGATGTGG-3′. The PCR products were run on 2% agarose gels and visualized by ethidium bromide staining.

2.10. Statistical analysis

Statistical analysis was performed using the PRISM (GraphPad Software Inc, San Diego, CA). Results are expressed as a mean ± SD. The one-way analysis of variance (ANOVA) was used for comparisons involving more than two groups. Statistical significance was defined as the conventional p-value of < 0.05.

3. Results

3.1. Effect of high glucose and palmitate-induced ROS generation and toxicity in H9c2 cells

Viability of H9c2 cells decreased in the condition of 30 mM high glucose (HG) and 250μM plamitate in MTT assay (Fig. 1A). In particular, the viability was significantly lowest in cells treated with both 30 mM glucose and palmitate (*vs.* 5 mM normal glucose control (NG), 30 mM high glucose, *** $P < .001$, ††† $P < .001$, respectively). Compared to 5 mM normal glucose, intracellular ROS generation of H9c2 cells increased in high glucose without significance (3.2 ± 0.5 fold), 250μM plamitate (4.0 ± 0.7 fold, **$P < .01$) and combination of high glucose and palmiate-treated condition (6.5 ± 0.4 fold, ***$P < .001$) with significance (Fig. 1B). The percentage of early and late apoptotic (AV- positive) cells in glucolipotoxic condition of palmitate in combination with high glucose (45.3 ± 22.1) was significantly increased than in 5 mM (2.1 ± 2.2, *$P < .05$) and 30 mM glucose (3.0 ± 3.3, † $P < .05$). (Fig. 1C, D).

3.2. Glucolipotoxicity-induced expressions of p53, Nrf2, NQO1 and cleaved caspase-3

For protein expression assessed by western blotting, whole lysates were used for p53, NQO1 and cleaved caspase-3, and nuclear extract for Nrf2. As shown in Fig. 2, when cells were incubated in the presence of palmitate and high glucose, p53 level was increased about 4-5 folds (*vs.* NG, HG, NG+palmitate, *** $P < .001$, ††† $P < .001$, ‡‡‡ $P < .001$, respectively) and cleaved caspase-3 level about 2.6 – 4.5 fold (*vs.* NG, HG, NG+palmitate, *** $P < .001$, ††† $P < .001$, ‡‡‡ $P < .001$, respectively). Compared to other conditions, Nrf2 expression showed increased tendency without significance, but NQO1 expression was decreased with significance in the presence of high glucose and palmitate (*vs.* HG † $P < .05$). To investigate the time course of gene expression and caspase-3 cleavage, we examined the protein expression of Nrf2, NQO1, p53, and cleaved caspase-3 at 3, 6, and 18 h. As shown in Fig. 3, glucolipotoxicity elicited Nrf2 expression, followed by expression of p 53. And then NQO1 expression was suppressed by activation of apoptotic p53 expression.

3.3. Effects of pifithrin-α (PFTα), a p53 inhibitor, on glucolipotoxicity-induced intracellullar ROS generation and toxicity in H9c2 cells

To explore the involvement of p53 in this apoptosis pathway, we examined the p53 protein expression using PFT-α, a p53 inhibitor. Apoptosis and viability was analyzed by western blot of cleaved caspase-3 and MTT assay, respectively. H9c2 cells exposed to combination of 30 mM glucose and 250μM palmiate showed increased p53 and cleaved caspase-3 expression (Fig. 4A), and showed significantly decreased cell viability (Fig. 4B) (*vs.* NG, HG, NG+palmitate, *** $P < .001$, ††† $P < .001$, ‡ $P < .05$, respectively) which was similar to Figs. 2A and 1A. Pre-treatment with 100μM PFT-α abrogated the expression of p53 and cleaved caspase-3 (Fig. 4A). PFT-α did not affect cell viability in the presence of normal or high glucose condition alone (NG vs NG+PFT-α, HG vs HG+PFT-α, both $p > 0.05$). PFT-α significantly decreased non-viable cells induced by high glucose and palmitate either alone or combination, but did not completely restore (*vs.* * for NG, † for HG, ‡ for NG+palmitate, § for HG+palmitate) (Fig. 4B, C). Similar findings were shown when H9c2 cells were knock-down by p53 siRNA (Supplementary Fig. 1). Interestingly, PFT-α did markedly restore NQO1 expression which was decreased by high glucose and palmiate (Fig. 4A), suggesting

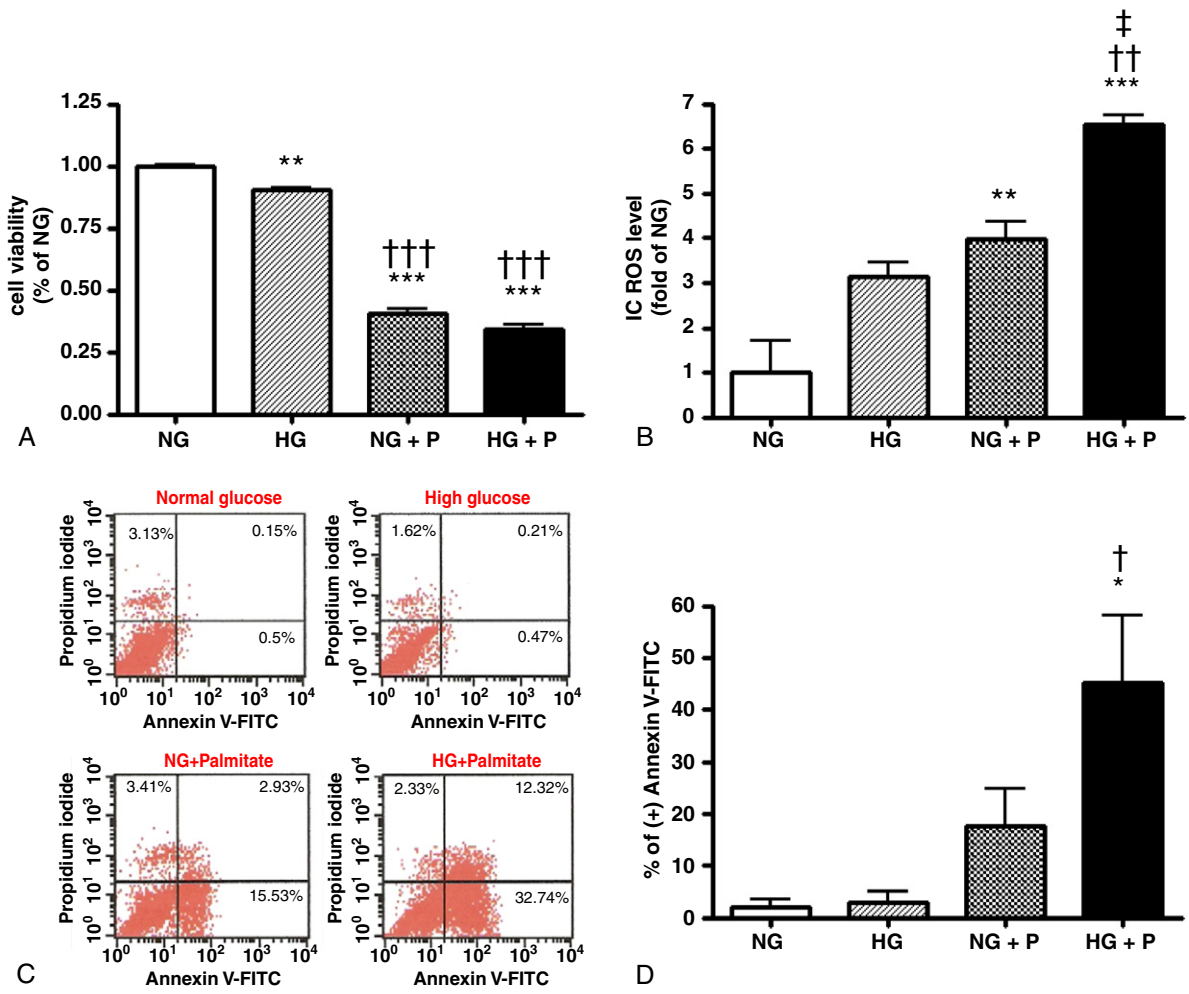

Fig. 1 – 30 mM high glucose and palmitate induced ROS generation and H9c2 cell toxicity. Cell viability assessed by MTT (A), intracellular ROS by flow cytometry following staining with H_2DCFDA (B), and cell apoptosis by FACS were measured (C, D). Bars indicate means ± SEM of three independent experiments. * $P < .05$, ** $P < .01$, *** $P < .001$ *vs.* NG (5 mM normal glucose)/ † $P < .05$, †† $P < .01$, ††† $P < .001$ *vs.* HG (30 mM high glucose)/ ‡ $P < .05$ *vs.* NG with 250μM plamitate.

a high sensitivity of endogenous expression of NQO1 to p53. In this regard, these results suggest that p53 is a key molecule in the glucolipotoxicity induced apoptosis through an inhibition of NQO1. In addition, 30 mM glucose and 250μM palmiate-treated H9c2 cells showed significant increased intracellular ROS generation (*vs.* NG, HG, NG +palmitate, *** $P < .001$, ††† $P < .001$, ‡‡‡ $P < .001$, respectively) which were similar to those shown in Fig.1B. Pretreatment with PFT-α (*vs.* HG+palmitate, all §§§ $P < .001$) significantly reduced intracellar ROS levels (Fig. 4D).

3.4. *p53 interacts with ARE-containing promoter of the NQO1 gene*

We demonstrated the possible binding of p53 with the NQO1 gene. A portion of the precleared chromatin was stored and labeled as input DNA (Fig. 4E number 1). The remaining chromatin was immunoprecipitated with IgG (Fig. 4E number 2), and p53 antibody (Fig. 4E number 3). As shown in Fig. 4E, the NQO1 promoter chromatin prepared from combination of high glucose and palmiate-treated H9c2 cells was immunoprecipitated with anti-p53 antibodies, thus indicating that this region interacts with p53.

3.5. *Effect of N-acetyl L-cysteines (NAC) on ROS generation and p53 expression*

To investigate the relationship between p53 expression and ROS, we repeated previous experiments shown in Fig. 4 with ROS scavenger N-acetyl-L-cysteins (NAC). Results of western blot of p53 and cleaved caspase-3, MTT, and intracellular ROS generation showed similar to Fig. 5. Pre-treatment with 1 mM NAC abrogated the expression of p53 and cleaved caspase-3 (Fig. 5A). NAC significantly decreased non-viable cells induced by high glucose and palmitate either alone or combination, but did not completely restore (Fig. 5B). Pretreatment with NAC (*vs.* HG+palmitate, all §§§ $P < .001$) significantly reduced intracellar ROS levels (Fig. 5C).

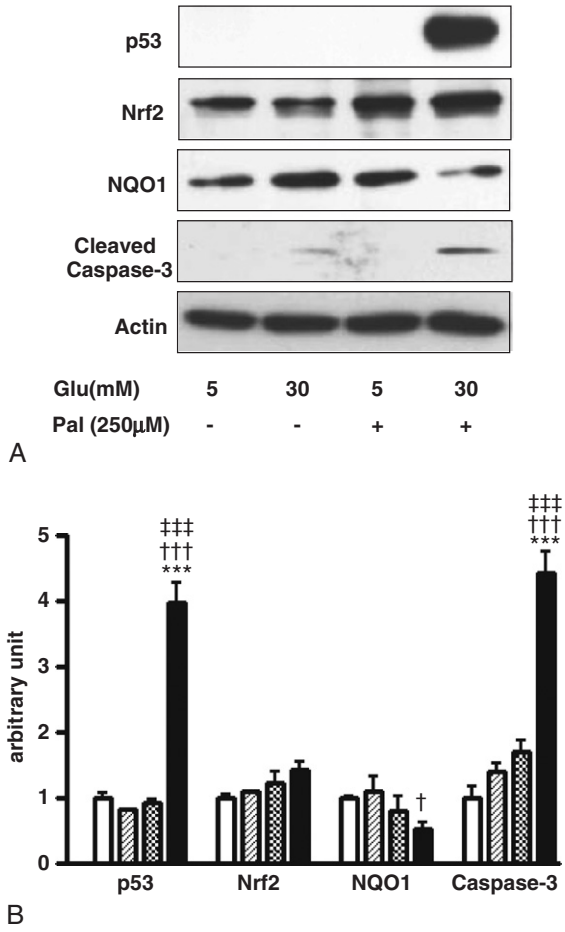

Fig. 2 – 30 mM high glucose and palmitate activated p53 and caspase-3 activity and decreased NQO1 expression. Levels of p53, Nrf2, NQO1 and caspase-3 expression were measured by western blotting. *** $P < .001$ *vs.* NG (5 mM normal glucose)/ † $P < .05$, ††† $P < .001$ *vs.* HG (30 mM high glucose)/ ‡‡‡ $P < .001$ *vs.* NG with 250μM plamitate.

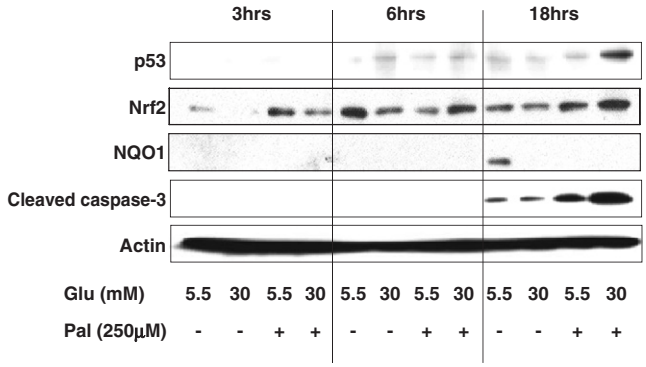

Fig. 3 – Time course of p53, Nrf2, NQO1, and cleaved caspase-3 expression. Levels of p53, Nrf2, NQO1 and caspase-3 expression were measured by western blotting at 3, 6, and 18 h.

4. Discussion

Oxidative stress increase in uncontrolled diabetic conditions and is likely involved in progression of cardiomyocytes and pancreatic β-cell dysfunction found in diabetes [8-10]. If metabolic glucolipotoxicity provokes intracellular environment toward oxidative stress, cells respond to activate the transcription of various antioxidant genes as well as apoptotic p53 activation, which induces cell cycle arrest [6]. In the present study, our attention was focused on the glucolipotoxicity-induced apoptosis of the cardiomyocyte and its apoptotic cell pathways. We hypothesized that glucolipotoxicity-induced apoptosis of H9c2 cells would be mediated through pro-apoptotic cross-talk of increased intracellular generation of ROS and expression of p53 as well as counteracting anti-apoptotic pathway through binding of p53 to its ARE promoters. To address this hypothesis, we demonstrated that high glucose in combination of palmitic acid consistently caused cardiomyobalst apoptosis (Fig. 1-5) which is consistent with the previous studies. Because concentrations of glucose above 10 mM are similar to a diabetic condition in vitro, 30 mM high glucose in our study is sufficient to develop diabetic condition. In contrast to palmitate-induced apoptosis in cardiomyobalst [1,11-15], there have been some disputes on the cell apoptosis induced by glucotoxicity alone, especially in cardiomyocyte [1,9,11]. Among those studies, glucotoxicity and lipotoxicity were synergistic in inducing apoposis in one study [11], but not in the other [1]. Taken together with our observations that 30 mM high glucose in the presence of 250μM palmitic acid induced apoptotic cell death and increased intracellular ROS levels in H9c2 cells (Fig. 1, 4, and 5), we suggest that glucolipotoxicity-induced cardiomyocyte apoptosis, referring to the synergistic, was triggered by intracellular ROS generation. One thing to note here is that palmitate alone did not significantly increase the inctracellular ROS levels (Fig. 4D and 5C). This result is consistent with previous report with neonatal rat cardiomyocytes [15]. It suggests that oxidative stress may not play an important role in palmitate-induced cell toxicity. Another consideration is possible off-target effects of PFTα. In Fig. 4 (A, B), although palmitate in condition of normal glucose did not induce p53, PFTα, a p53 inhibitor, significantly ameliorated cell viability of palmitate-treated cells.

Second, in concordance with previous reports, we found that glucolipotoxicities activated intracellular ROS, resulting in, at least in part, increases of p53 and cleaved caspase-3 expression in H9c2 cells. The tumor suppresser protein p53 is a transcription factor that is well known to either growth arrest or apoptosis [16,17]. It have been well demonstrated that accumulation of high levels of ROS can induce p53 expression by inducing of DNA damage in many studies [12,13]. DNA damage-dependent activation of p53 also induces a significant accumulation of ROS that is crucial for the p53-dependent apoptosis [18]. Interestingly, in this study, p53 expression was not affected by glucotoxicity or lipotoxicity alone but markedly increased by synergistic glucolipotoxicity (Fig. 2-5). It suggests that p53 expression might be responsive only to a high level of ROS in cross-talk manner. In our study, treatment of NAC concomitantly abrogated both p53 expression and intracellular ROS levels, and addition of PFT-α, an inhibitor of p53, markedly lowered intracellular level of ROS (Fig. 4D). Based on previous studies and our results, it is likely that a positive

feedback loop might be run in the cycle, in which glucolipotoxicity-induced intracellular ROS generation stimulates p53 expression which, in return, induces an accumulation of ROS. Based on the effects of NAC and PFT-α on ROS levels, p53 and caspase-3 expression in this study (Fig. 4 and 5), p53-dependent or mediated glucotoxicity might plays an important role in development of cardiomyocyte apoptosis.

Third, we additionally investigated the p53 mediated glucolipotoxicity-induced apoptosis of rat cardiomyoblast cell through inhibiting anti-apoptosis pathway of Nrf2-NQO1

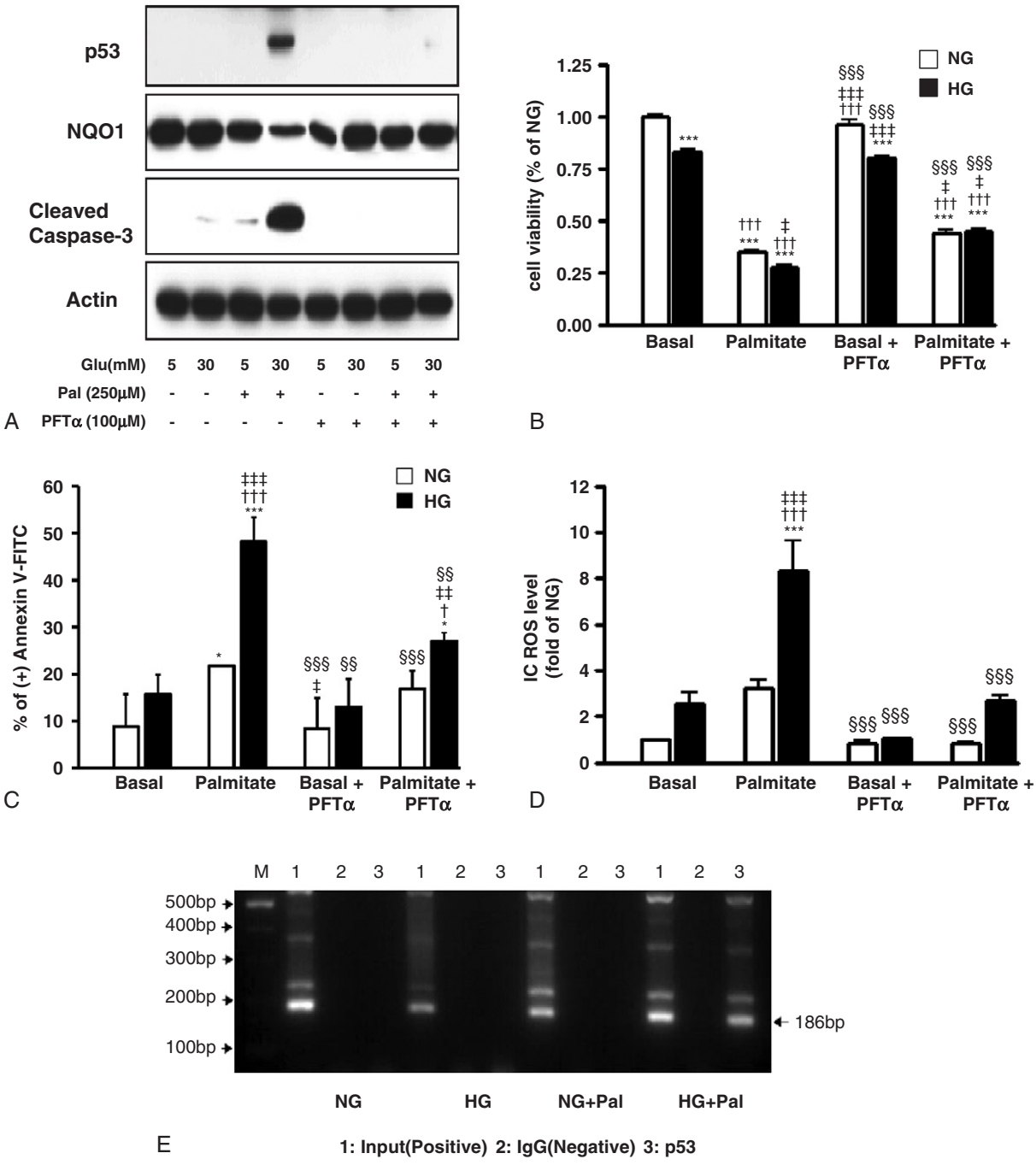

Fig. 4 – PFTα, a p53 inhibitor, abrogated the ROS production. H9c2 cell viability increased and apotosis decreased by PFTα. p53 interacted with ARE-containing promoter of the NQO1 gene. Levels of p53, NQO1 and caspase-3 expression evaluated by western blotting (A), cell viability by MTT (B), cell apoptosis by FACS (C), and intracellular ROS by flow cytometry following staining with H_2DCFDA (D) were measured. * $P < .05$, *** $P < .001$ *vs.* NG (5 mM normal glucose)/ † $P < .05$, ††† $P < .001$ *vs.* HG (30 mM high glucose)/ ‡ $P < .05$, ‡‡ $P < .01$, ‡‡‡ $P < .001$ *vs.* NG with 250μM plamitate/ §§ $P < .01$, §§§ $P < .001$ *vs.* HG with 250μM plamitate. The NQO1 promoter chromatin prepared from combination of high glucose and palmiate-treated H9c2 cells was immunoprecipitated with anti-p53 antibodies (E). Input DNA (number 1), IgG (number 2), p53 antibody (number 3).

signaling. In previous reports [6,19], low levels of p53 expression seem to activate the several antioxidant genes resulting in consequent decrease of intracellular ROS. However, high levels of p53 expression suppress the Nrf2-induced transcription of ARE-containing promoters. Nrf2 dissociation from Keap1 activated antioxidant genes such as NQO1, glutathione s-transferase, and r-glutamylcysteine synthase, which are transactivated by binding to ARE regions of their promoters [6]. In this study, as shown in Fig. 2-5, Nrf2-dependent activation of antioxidant genes, such as NQO1 is down-modulated by p53 overexpression. This was also well demonstrated in the results of time couse experiments (Fig. 3). As shown in Fig. 4E, p53 binds to ARE regions of NQO1 promoter assessed by chromatin immunoprecipitation. In these regards, despite of increased expression of Nrf2 under the condition of cell stress, p53 apparently represses the Nrf2 transcriptional activity by displacing Nrf2 bound to the NQO1 promoter which results in further p53-dependent apoptosis. However, this glucolipotoxicity-induced p53-dependent apoptotic pathway could not fully contribute to the development of cardiomyocyte cell death because NAC and PFT-α could partially hinder the induction of cardiomyoblast apoptosis. In addition, there are many antioxidant enzymes against increased ROS, which are regulated by Nrf2. In this study, we only investigated the expression of NQO1. Other antioxidant enzymes, such as heme oxygenase-1 and glutathione S-transferase, might play a role in this apoptotic pathway. Although these findings, we still have some limitations in our study. We used H9c2 cells as cardiomyocytes. In this immortalized cell line, it is possible that the function of p53 might be impaired or deranged. The primary cardiomyocytes will be helpful to confirm this mechanism.

In summary, 30 mM high glucose in the presence of 250μM palmitic acid induced apoptotic cell death. The p53-dependent or mediated glucotoxicity might play an important role in development of cardiomyocyte apoptosis through dual pathways: stimulating pro-apoptosis signaling as well as suppressing anti-apoptosis pathway of Nrf2-NQO1 signaling.

Supplementary materials related to this article can be found online at doi:10.1016/j.metabol.2011.09.005.

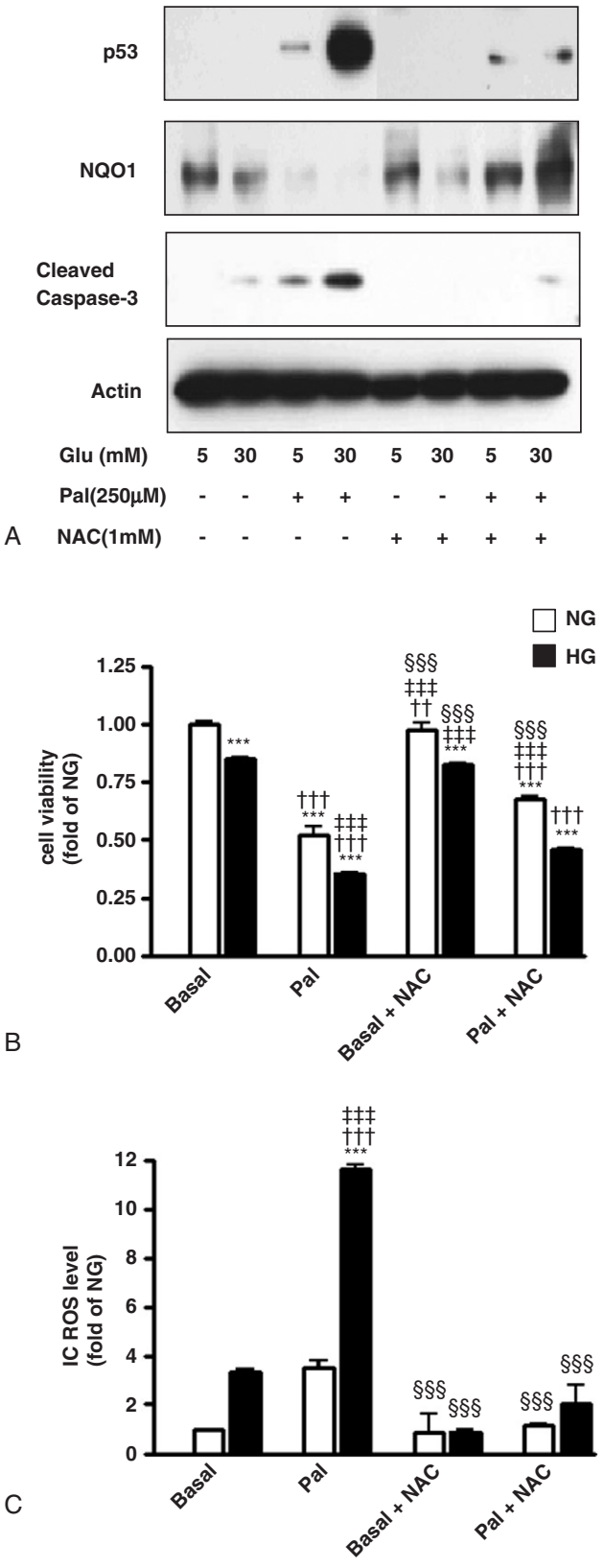

Fig. 5 – NAC abrogated the ROS production and increased H9c2 cell viability. Levels of p53, NQO1 and caspase-3 expression evaluated by western blotting (A), cell viability by MTT (B), and intracellular reactive oxygen species (ROS) by flow cytometry following staining with H_2DCFDA (C) were measured. *** $P < .001$ *vs.* NG (5 mM normal glucose)/ †† $P < .01$, ††† $P < .001$ *vs.* HG (30 mM high glucose)/ ‡‡‡ $P < .001$ *vs.* NG with 250μM plamitate/ §§§ $P < .001$ *vs.* HG with 250μM plamitate.

Funding

This study was supported by grants from the Korean Diabetes Association (2007).

Conflict of Interest

The authors report no conflicts of interest. The authors alone are responsible for the content and writing of the paper.

REFERENCES

[1] Dyntar D, Eppenberger-Eberhardt M, Maedler K, et al. Glucose and palmitic acid induce degeneration of myofibrils and modulate apoptosis in rat adult cardiomyocytes. Diabetes 2001;50:2105-13.

[2] Listenberger LL, Ory DS, Schaffer JE. Palmitate-induced apoptosis can occur through a ceramide-independent pathway. J Biol Chem 2001;276:14890-5.

[3] Fiordaliso F, Leri A, Cesselli D, et al. Hyperglycemia activates p53 and p53-regulated genes leading to myocyte cell death. Diabetes 2001;50:2363-75.

[4] Wang S, Leonard SS, Ye J, et al. The role of hydroxyl radical as a messenger in Cr(VI)-induced p53 activation. Am J Physiol Cell Physiol 2000;279:C868-75.

[5] Qiu T, Xie P, Liu Y, et al. The profound effects of microcystin on cardiac antioxidant enzymes, mitochondrial function and cardiac toxicity in rat. Toxicology 2009;257:86-94.

[6] Faraonio R, Vergara P, Di Marzo D, et al. p53 suppresses the Nrf2-dependent transcription of antioxidant response genes. J Biol Chem 2006;281:39776-84.

[7] Spector AA. Structure and lipid binding properties of serum albumin. Methods Enzymol 1986;128:320-39.

[8] Kim WH, Lee JW, Suh YH, et al. AICAR potentiates ROS production induced by chronic high glucose: roles of AMPK in pancreatic beta-cell apoptosis. Cell Signal 2007;19:791-805.

[9] Cai L, Li W, Wang G, et al. Hyperglycemia-induced apoptosis in mouse myocardium: mitochondrial cytochrome C-mediated caspase-3 activation pathway. Diabetes 2002;51:1938-48.

[10] Barter PJ. The Causes and Consequences of Low Levels of High Density Lipoproteins in Patients with Diabetes. Diabetes Metab J 2011;35:101-6.

[11] Ghosh S, An D, Pulinilkunnil T, et al. Role of dietary fatty acids and acute hyperglycemia in modulating cardiac cell death. Nutrition 2004;20:916-23.

[12] Kong JY, Rabkin SW. Lovastatin does not accentuate but is rather additive to palmitate-induced apoptosis in cardiomyocytes. Prostaglandins Leukot Essent Fatty Acids 2002;67:293-302.

[13] Miller TA, LeBrasseur NK, Cote GM, et al. Oleate prevents palmitate-induced cytotoxic stress in cardiac myocytes. Biochem Biophys Res Commun 2005;336:309-15.

[14] Miller TA, Icli B, Cote GM, et al. Palmitate alters neuregulin signaling and biology in cardiac myocytes. Biochem Biophys Res Commun 2009;379:32-7.

[15] Hickson-Bick DL, Sparagna GC, Buja LM, et al. Palmitate-induced apoptosis in neonatal cardiomyocytes is not dependent on the generation of ROS. Am J Physiol Heart Circ Physiol 2002;282:H656-64.

[16] Waldman T, Kinzler KW, Vogelstein B. p21 is necessary for the p53-mediated G1 arrest in human cancer cells. Cancer Res 1995;55:5187-90.

[17] Villunger A, Michalak EM, Coultas L, et al. p53- and drug-induced apoptotic responses mediated by BH3-only proteins puma and noxa. Science 2003;302:1036-8.

[18] Polyak K, Xia Y, Zweier JL, et al. A model for p53-induced apoptosis. Nature 1997;389:300-5.

[19] Sablina AA, Budanov AV, Ilyinskaya GV, et al. The antioxidant function of the p53 tumor suppressor. Nat Med 2005;11:1306-13.